

An α -MN collateral to γ -MNs can mitigate velocity-dependent stretch reflexes during voluntary movement: A computational study

Grace Niyo¹, Lama I Almofeez¹, Andrew Erwin^{2,3}, Francisco J Valero-Cuevas^{1,2,†,*}

1 Biomedical Engineering Department, University of Southern California, Los Angeles, CA, USA

2 Biokinesiology and Physical Therapy Department, University of Southern California, Los Angeles, CA, USA

3 Mechanical and Materials Engineering Department, University of Cincinnati, Cincinnati, OH, USA

†Senior author. * valero@usc.edu

Keywords: Alpha, gamma, beta motoneurons, motoneurons, neuromuscular control, computational neuroscience, neural control of movement, muscle spindles, muscle afferentation, neuromechanics, collateral projections, spinal cord

Abstract

The primary motor cortex does not uniquely or directly produce α -MN drive to muscles during voluntary movement. Rather, α -MN drive emerges from the synthesis and competition among excitatory and inhibitory inputs from multiple descending tracts, spinal interneurons, sensory inputs, and proprioceptive afferents. One such fundamental input is velocity-dependent stretch reflexes in lengthening (antagonist) muscles, which are thought to be inhibited by the shortening (agonist) muscles. It remains an open question, however, the extent to which velocity-dependent stretch reflexes disrupt voluntary movement, and whether and how they are inhibited in limbs with numerous mono- and multi-articular muscles where agonist and antagonist roles become unclear and can switch during a movement. We used a computational model of a *Rhesus Macaque* arm to simulate movements with feedforward α -MN commands only, and with added velocity-dependent stretch reflex feedback. We found that velocity-dependent stretch reflex caused movement-specific, typically large and variable disruptions to the arm endpoint trajectories. In contrast, these disruptions became small when the velocity-dependent stretch reflexes were simply scaled by the α -MN drive to each muscle (equivalent to an α -MN excitatory collateral to its homologous γ -MNs, but distinct from $\alpha - \gamma$ co-activation). We argue this circuitry is more neuroanatomically tenable, generalizable, and scalable than $\alpha - \gamma$ co-activation or movement-specific reciprocal inhibition. We propose that this mechanism at the homologous propriospinal level, by locally and automatically regulating the highly nonlinear neuro-musculo-skeletal mechanics of the limb, could be a critical low-level enabler of learning, adaptation, and performance via cerebellar and cortical mechanisms.

Significance

The problem of muscle afferentation has long been an unsolved problem, and a foundation of voluntary motor control. How unmodulated velocity-dependent stretch reflexes disrupt voluntary movement and how they should be inhibited in limbs with numerous mono- and multi-articular muscles remain unclear. Here we demonstrate the cost of unregulated velocity-dependent reflexes, and propose a low-level propriospinal mechanism that can regularize these errors and enables motor learning and performance. Our results suggest that this spinal level mechanism of scaling dynamic γ -MN by the homologous α -MN collateral provides a generalizable mechanism that could be a low-level enabler of accurate and predictable movements that locally stabilizes and complements the synthesis and competition among cortical, subcortical or propriospinal projections to α -MN pools

Introduction

Muscle spindle afferent signals contribute to the proprioceptive feedback signals that are important for kinesthesia, posture, balance [1–3], muscle tone [4], and control of voluntary movement [2, 5]. The monosynaptic stretch reflex

1
2
3

loop includes muscle spindles and their associated Ia and II afferent sensory neurons, which sense muscle fiber velocity and length. Additionally, it involves fusimotor $\gamma_{dynamic}$ and γ_{static} motoneurons that innervate intrafusal muscle fibers, regulating muscle spindle sensitivity [6–8]. It is often suggested that dysregulation of the monosynaptic stretch reflex loop is responsible for movement disorders such as hyperreflexia, spasticity, dystonia, etc. [9, 10]. However, the regulation and contribution of this fusimotor system to voluntary movements and movement pathologies remain debatable [10].

Understanding the fusimotor system has been difficult due to the experimental challenges of recording from $\gamma_{dynamic}$ and γ_{static} motoneurons in behaving animals and humans [11–16]. As a result of these difficulties, muscle spindle afferent signals are most commonly studied and described for single-joint systems with clear agonist-antagonist muscle pairs (figure 35-5 in [17, 18]).

Importantly, the velocity-dependent Ia signal can—if not regulated or inhibited—be considered a form of ‘internal perturbation’ where stretch reflexes in eccentrically contracting (i.e., antagonist) muscles can disrupt or stop joint rotations induced by the concentrically contracting muscles [4, 8, 19, 20]—and compromise movement accuracy. It is in this context that Sherrington mentioned that ‘*Inhibition is as important as excitation*’ [4]: in single-joint movements driven by an agonist-antagonist muscle pair, reciprocal inhibition of the antagonist α -MNs provided by Ia inhibitory interneuron mitigate the disruption of voluntary movements [18, 21]. However, this simplified conceptual framework for reciprocal inhibition is difficult to extend and generalize to limbs driven by numerous multi-articular muscles where the roles of agonist and antagonist become unclear and can change during the movement [19, 20, 22, 23].

In this study, we apply first principles to address two issues. First, in what ways do positive homologous muscle velocity feedback (i.e., velocity-dependent stretch reflexes) perturb limb movements in the general case of numerous multi-articular muscles? And second, would spinal modulation of velocity-dependent stretch reflex gains—in the spirit of Sherrington—mitigate these disruptions?

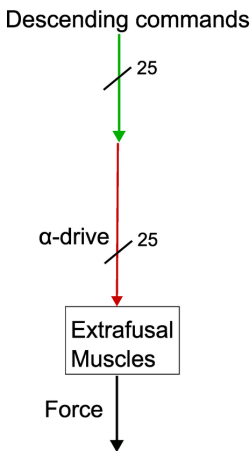
We find that unmodulated, physiologically tenable monosynaptic velocity-dependent stretch reflexes do, in fact, disrupt voluntary movements in significant, variable and task-specific ways. However, scaling the stretch reflex gain by (i) the level of the postsynaptic homologous α -MN drive or (ii) pre-synaptic $\alpha - \gamma$ co-activation greatly reduces disruptions for most, but not all, voluntary movements.

Methods

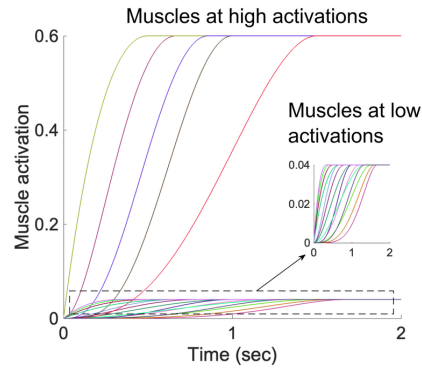
Open-loop simulation of arm movements without feedback

We created 1,100 open-loop three-dimensional arm movements of a Rhesus Macaque (*Macaca mulatta*) arm model, each lasting two seconds with a 2000 sampling rate. The model was adapted from the SIMM (Musculographics Inc) model developed by Moran et al. [24] into a MuJoCo model (**M**ulti-**J**oint dynamics with **C**ontact) by first loading the SIMM model into an OpenSim (Open Source Simulation and Modeling) model [25] and then converting the OpenSim model into MuJoCo [26]. While the original model has 38 muscles and 7 degrees of freedom (DoF), we excluded hand muscles and fixed the wrist joint as they are unnecessary for the simulated upper arm movements. The adapted MuJoCo model is shown in (Fig.1C) with the same body segment lengths, joints, and tendon routing as the original model, 25 muscles and 5 DoF (shoulder abduction/adduction, shoulder flexion/extension, shoulder rotation, elbow flexion/extension, and forelimb pronation/supination). The muscletendon model is a Hill-type with inelastic tendons [27] and the same muscle force parameters, tendon slack lengths as in the original model. During open-loop simulations, each of the 25 Hill-type muscles was controlled by a single α -MN drive. Each muscle received a feed-forward α -MN drive signal (Fig.1A), whose level could vary from 0 to 1, which we refer to as 0% to 100% muscle activity. The feed-forward α -MN drives were created as a beta probability density function to generate beta shapes which then were scaled and transformed into ramp signals that for five randomly-selected muscles reached 60% of maximum, while the remaining 20 muscles reached only 4% of maximum muscle activity (Fig.1B). This distribution of high and low activations mitigated co-contraction and enabled both small and large arm movements with maximal endpoint displacements ranging 5.178 cm to 6.872 cm that spanned the full workspace of the 47.35 cm length arm model (S1 Fig). The trajectory of the endpoint (distal head of the third metacarpal) of the open-loop arm movements served as reference endpoint trajectories (Fig.1C) for computing deviations of the endpoint trajectory of arm movement with velocity-dependent stretch reflex feedback from the open-loop endpoint trajectories.

A. Open-loop simulation



B. Baseline Activation Signals



C. Reference Endpoint Trajectory

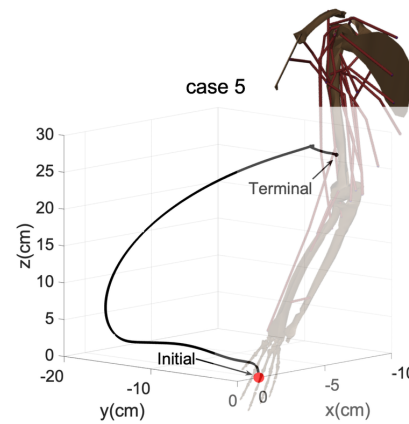


Fig 1. Sample time history of open-loop α -motoneuron activations to muscles to produce endpoint trajectory (case 5 out of 1,100). B) For each open-loop movement, five randomly-selected muscles were activated from zero to 60% of maximum following a random ramp-shaped activation profile, while the remaining 20 muscles reached only 4% of maximum in a similar way (inset) to prevent excessive co-contraction and enable large movements throughout the workspace of the limb. C) The ensuing reflex-free reference trajectory of the endpoint (distal head of the third metacarpal) for the sample activations in B is shown (black trace) from the initial position (red dot) to the terminal position (black dot).

Closed-loop simulation of arm movements with velocity-dependent stretch feedback

Excitatory velocity-dependent (Ia afferent) stretch reflexes from muscle spindles form feedback loops to homologous alpha-motoneurons of the extrafusal muscle via spinal pathways [18]. We added a simple muscle spindle model to each of the 25 Hill-type muscles of the macaque arm. The model takes muscles velocity input and generates Ia afferent as positive muscle velocity (i.e., velocity-dependent stretch reflex) output. For each of the 1,100 arm movements, we performed closed-loop simulations of the movement with the velocity-dependent stretch reflex feedback of different reflex gain k from 1 to 10. We show these gains are physiologically tenable by computing peak change in muscle activation caused by the velocity-dependent (Ia afferent) stretch reflex feedback and compare them to reflexes elicited in human arms (up to 40%MVC reflex EMG) during interactions with destabilizing environments [28]. A schematic overview of the closed-loop simulation of movements with velocity-dependent stretch reflex feedback is shown in figure 2. The α -drive of each muscle received the same feedforward α -MN drive as during the open-loop simulation. At each simulation time step, the muscle spindle generated the velocity-dependent stretch reflex feedback ($k * v_{stretch}$) modulated at gain k to the homologous α -drive. The muscle activation was computed as follows:

$$a_m(t) = a_{ref}(t) + k * v_{stretch}(t) \quad (1)$$

Where $a_{ref}(t)$ refers the feedforward α -MN drive at time t and $v_{stretch}$ is positive muscle velocity v_m for lengthening muscles and zero for shortening or isometrically contracting muscles.

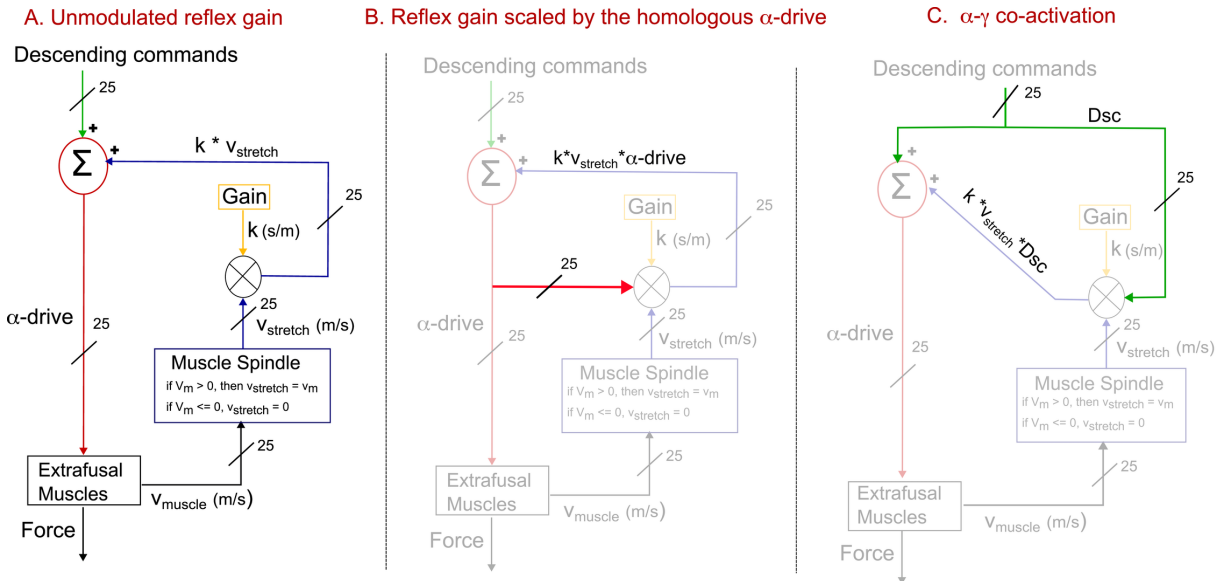


Fig 2. Schematic view of the closed-loop simulation of movements with velocity-dependent stretch reflex feedback. During closed-loop simulation, the feedforward α -MN drive was the same as the feedforward α -MN drive of open-loop arm movements (Fig.1A) for both unmodulated reflex gain (A) and reflex gain proportional to the α -drive (B). The muscle spindle of each muscle received the muscle velocity (V_m) as input and generated the stretch velocity of the muscle ($V_{stretch}$) as positive muscle velocity for when the muscle was lengthening or zero for when shortening (i.e., negative velocity) or isometrically contracting. For the unmodulated reflex gain (A), the muscle stretch velocity was multiplied by a reflex gain k to produce the velocity-dependent stretch reflex feedback ($k * V_{stretch}$), while in (B), the reflex gain was simply scaled to the α -drive (red bold arrow) to produce velocity-dependent stretch reflex feedback with reflex gains proportional to the muscle's α -drive ($k * V_{stretch} * \alpha$ -drive). Each closed-loop simulation was simulated for all 1,100 arm movements at reflex gain k values from 1 to 10 in steps of 1. Examples of endpoint trajectories of arm movements for unmodulated reflex gains and reflex gains proportional to the α -drive are shown in Fig.3& Fig.4

We scaled the stretch reflex gain k to the α -drive of the muscle (fig.2B) to investigate how the disruption in the endpoint trajectories change when the stretch reflex gain is proportional to the ongoing muscle activation signal. In this closed-loop simulation the muscle activation was computation using the following equations:

$$a_m(t) = a_{ref}(t) * (1 + k * v_{stretch}(t)) \quad (2)$$

Similar to open-loop simulations, we recorded trajectories of the endpoint at each gain k and computed deviation in the movement trajectory (i.e., cumulative residual, CR) and deviation in of terminal position (i.e., terminal error, TE) of the endpoint trajectories from their reference endpoint trajectory of the open-loop arm movement. CR is the mean of the Euclidean deviations in the movement trajectory (Eq.3) and TE is the deviation of the terminal position of the endpoint Eq.4.

$$RE = \frac{\sum_{t=0}^2 \sqrt{(x(t)_\alpha - x(t)_{\alpha+Ia})^2 + (y(t)_\alpha - y(t)_{\alpha+Ia})^2 + (z(t)_\alpha - z(t)_{\alpha+Ia})^2}}{N} \quad (3)$$

$$TE = \sqrt{(x(t_f)_\alpha - x(t_f)_{\alpha+Ia})^2 + (y(t_f)_\alpha - y(t_f)_{\alpha+Ia})^2 + (z(t_f)_\alpha - z(t_f)_{\alpha+Ia})^2} \quad (4)$$

The x,y,z positions of the endpoint for open-loop arm movements (i.e., movements without feedback) are $x(t_f)_\alpha$, $y(t_f)_\alpha$, $z(t_f)_\alpha$ and $x(t_f)_{\alpha+Ia}$, $y(t_f)_{\alpha+Ia}$, $z(t_f)_{\alpha+Ia}$ are x, y, and z positions of movement with velocity-dependent (Ia afferent) feedback for a specified reflex gain k , and N is the the number of samples. The magnitude of the disruption of the arm endpoint trajectory at each gain was quantified by scaling CR and TE of each movement to its to maximal endpoint displacement (S1 Fig).

Results

We used closed-loop simulations of a 25-afferented Hill-type muscles and 5 DOF model of a Rhesus macaque monkey to study how uninhibited velocity-dependent stretch reflexes disrupt arm movement trajectory and how the disruptions changes when the reflex gain is increased. The afferented muscle consists of a simple muscle spindle model that outputs positive velocity of lengthening muscles (i.e., velocity of stretch) as afferent feedback subject to a reflex gain. The peak change in muscle activation at any reflex gain (S2 Fig) were comparable to those (up to 40% MVC) observed in the human arm during interactions with destabilizing environments [28]. We further investigated how the disruption in movement trajectory change when reflex gains are simply proportional to the α -drive to muscle. Using our neuromuscular computational model, we find that the disruptions of the arm endpoint trajectories were surprisingly movement-specific, typically large and variable, and could even change movement direction as the reflex gain increased (Fig.3A). In contrast, these disruptions became small at all reflex gains when the simulated stretch reflexes were made proportional to the α -MN drive to muscles (Fig.3B).

Unmodulated velocity-dependent stretch reflexes cause large, variable disruptions of the endpoint trajectory in task-dependent ways

Our 1,100 open-loop simulations of arm endpoint trajectories resulted in small and large arm movements (S1 Fig), which were disrupted when closing the loop with the velocity-dependent stretch reflex feedback. Unmodulated reflex gains resulted in disrupted movement trajectories (Fig. 3A, cases 635, 147, 430, 884, and 122). Conversely, in other arm movements, the terminal positions remained unaffected by the reflex gains (Fig. 3A, cases 5,518 and 596). Additionally, further increase in reflex gain could change the movement direction (Fig.3A), case 884 and 122). In all arm movements, disruption in the endpoint trajectory increased when the reflex gain was increased; however, at any reflex gain, k , the magnitude of disruption in the endpoint trajectory were different within movements. This shows that the disruption in the arm endpoint trajectory depended the stretch reflex gain and the movement itself.

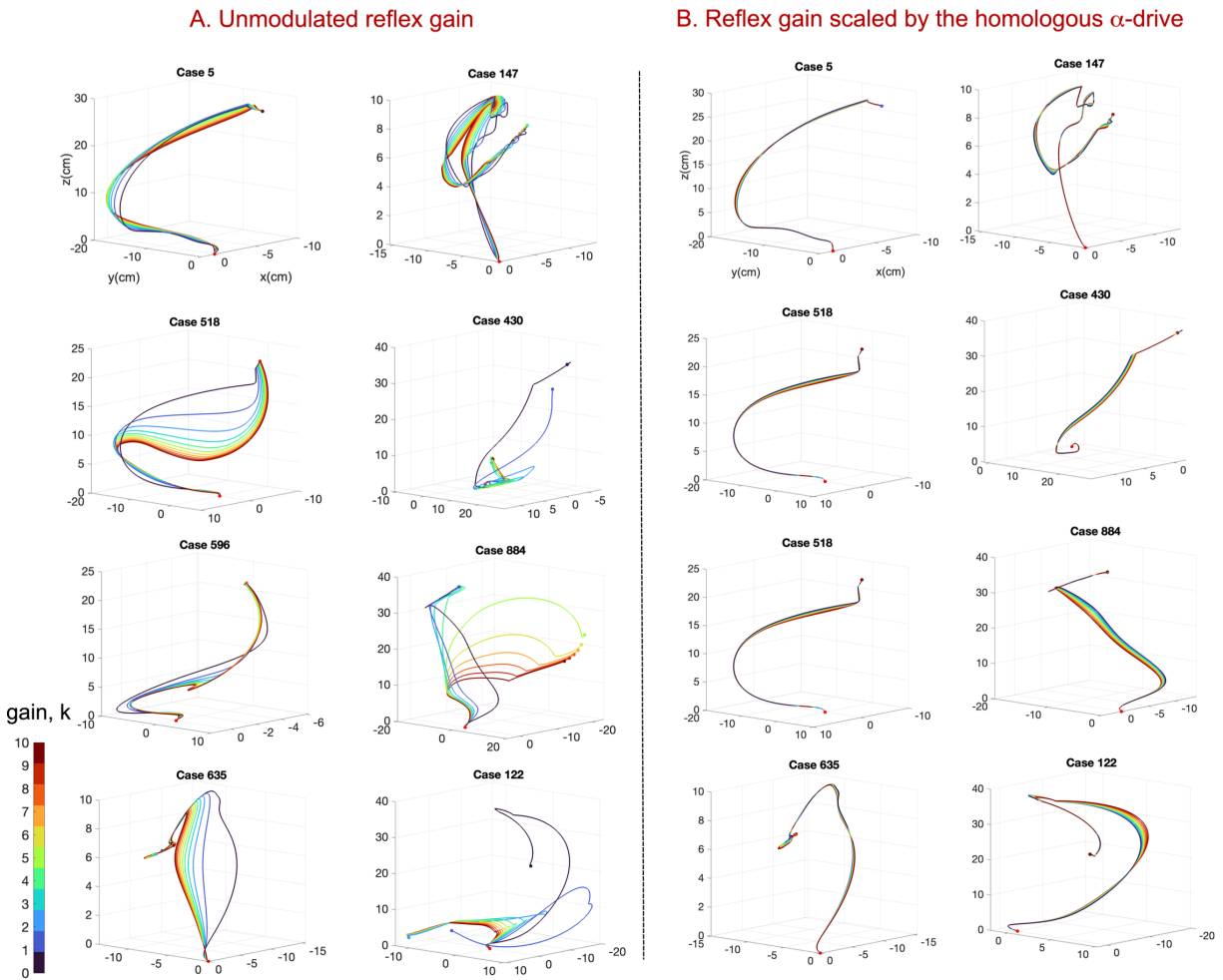


Fig 3. Unmodulated reflex gains are cause large, variable disruptions in the movement endpoint.(A) Fourteen examples of the 1,100 arm movements with unmodulated reflex gains show that increasing the reflex gain progressively disrupts the endpoint trajectory in different ways. In (A) cases 5, 518 and 596 only the movement trajectories were disrupted. In (A) cases 635, 147, 430, 884, and 122, both the movement trajectory and terminal position were disrupted; however, in cases 884 and 122, increasing the reflex gain k changed the movement direction. (B) The same fourteen endpoint trajectories in (A), but the reflex gain was proportional to the α -drive to the muscle (see details in Fig.2B of Methods), show that the disruption in the endpoint trajectories were small at all reflex gain k . The endpoint trajectory of open-loop movement is the black plot at reflex gain k of 0. Further analysis of the effects of velocity-dependent on all 1,100 arm movements at each reflex gain is shown figure 5.

The definition of agonist and antagonist muscles loses meaning when considering biologically plausible models of the upper limb (as opposed to single degree of freedom movements primarily considered in the literature) with multiple joints and multi-articular muscles as in our macaque arm model. Instead of reciprocal inhibition of reflexes—which has been historically studied in reduced models [18,21]—we proportionally modulated the reflex gain by the α -drive to the muscle (Fig.2B)). In this closed-loop simulation of arm movements with reflex gain k proportional to individual muscle's α -drive, the disruption in the movement endpoint trajectory became small in each movement at all reflex gains(Fig.3B). In figure4, we show four examples of endpoint trajectories that had larger disruptions when the reflex gain was scaled by the homologous α -drive (bottom plots). These disruptions were still small compared to the unmodulated reflex gains (top plots).

A. Unmodulated reflex gain B. Reflex gain scaled by the homologous α -drive

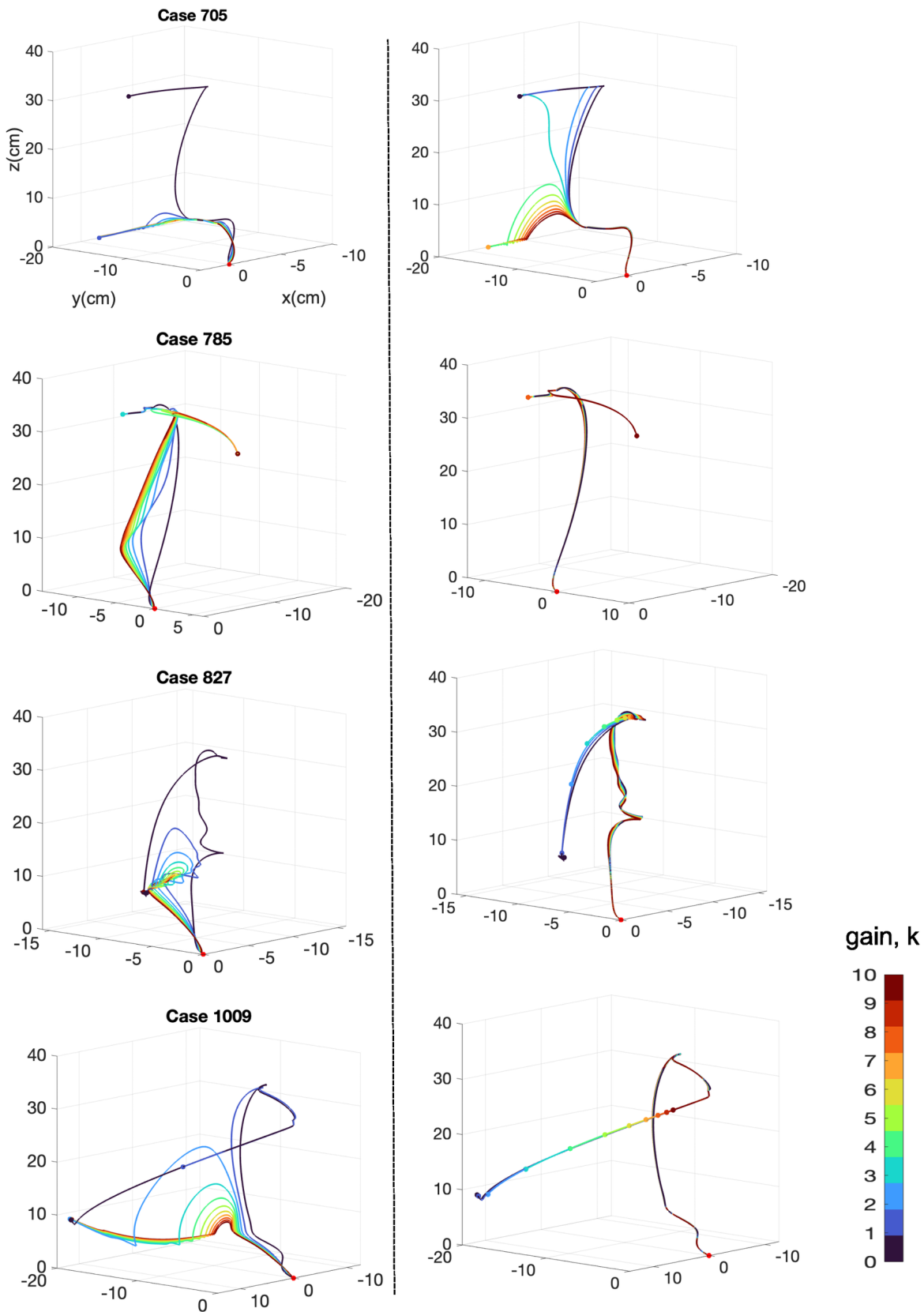


Fig 4. The largest endpoint disruption when the reflex gain was made proportional to the α -drive of the muscle were smaller than the disruptions in the arm movements with unmodulated reflex gains. (B) Four examples of endpoint trajectories of the arm movements with the largest disruption in the endpoint trajectory when the reflex gain was made proportional to the alpha drive of the muscle and (A) their respective endpoint trajectories when the reflex gain were unmodulated.

We also simulated $\alpha - \gamma$ co-activation and compared the overall distribution of the disruptions in the endpoint movement trajectory (i.e., cumulative residual Fig.5,top plots) and the terminal position (i.e., terminal error Fig.5,bottom plots) at each reflex gain (vertical scatter plots). The cumulative residual and terminal error were large at higher reflex gains. However, the magnitude of disruptions at any gain k were small and less variable when the stretch reflexes were scaled by the α -drive Fig.5B) or when simulating $\alpha - \gamma$ co-activation (Fig.5C). Figure 6 shows the error when reflex gain was scaled by the α -drive vs simulating $\alpha - \gamma$ co-activation .

111
112
113
114
115
116

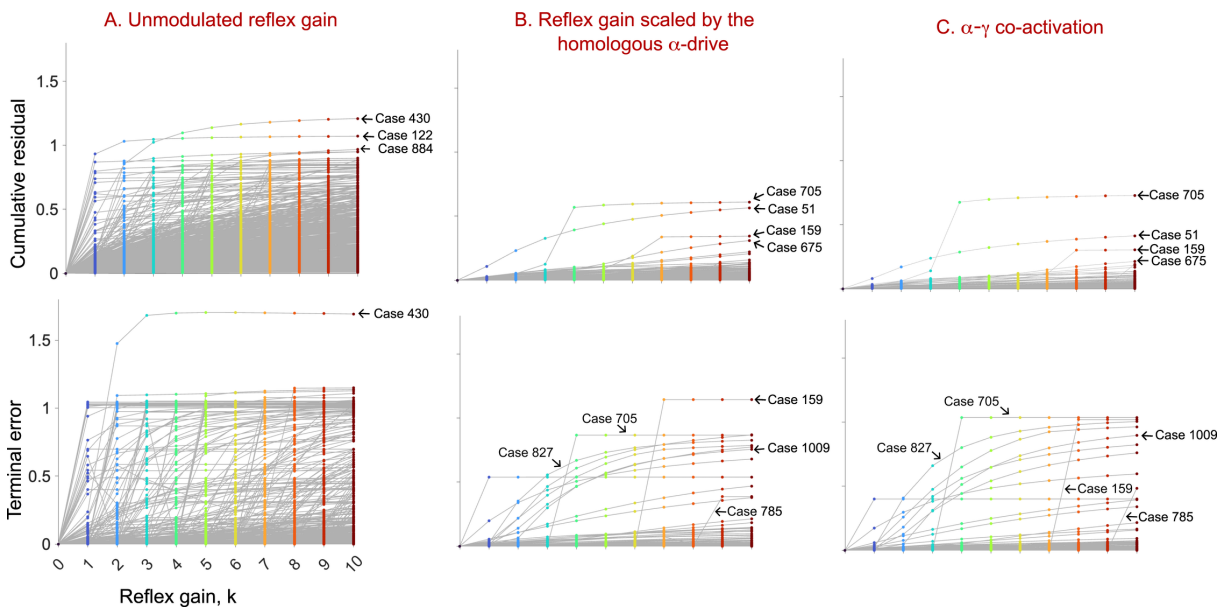


Fig 5. Terminal error and cumulative residual with respect to the reference trajectories were large and variable for the unmodulated stretch reflex gains(A); but typically small to negligible when the stretch reflexes were scaled to the baseline activation level of each muscle (B). For each movement, we divided the deviation in movement trajectory (i.e., cumulative residual, CR) and terminal position (i.e., terminal error) by the maximal endpoint displacement of that movement's reference trajectory (S1 Fig). Both CR and TE (top and bottom plots respectively) of all 1,100 arm movements at each gain k reduced when the reflex gains were proportional to the α -drive (B) compared to the unmodulated reflex gains(A). In (C), we made the reflex gain proportional to the feedforward α -MN drive (similar to the $\alpha - \gamma$ co-activation theory). Similar to when the reflex were proportional the α -drive collateral (B), CR and TE became small compared to the unmodulated reflex gain in (A). The physiological plausibility of modulating reflex gain at the spinal level(B) vs the $\alpha - \gamma$ co-activation(C) is provided in discussion session.

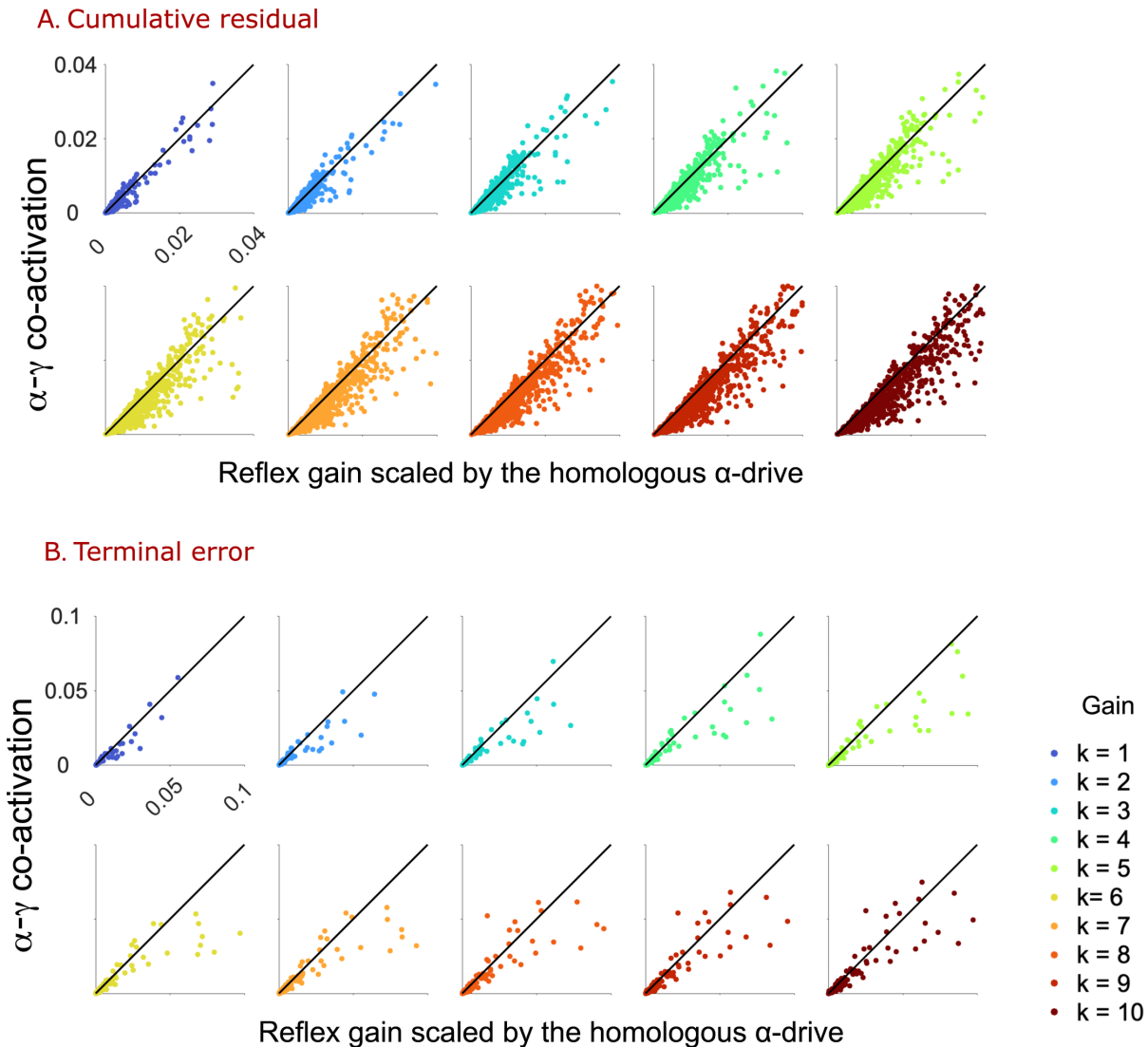


Fig 6. Cumulative residual (A) and terminal error (B) when simulating ideal $\alpha - \gamma$ co-activation vs. a simple homologous circuit where reflex gain was scaled by the α -drive (Fig. 8). Note these plots, for clarity, these plots show cumulative residual and terminal error shown in Fig.5B&C up to 0.04 and 0.1 respectively.

Discussion

We used a computational model of a *Rhesus Macaque* arm with 25 muscles to test whether velocity-dependent stretch reflexes (i.e., simple positive feedback monosynaptic simulating Ia afferents) are sufficiently disruptive to require active or predictive modulation to produce accurate movements in realistic multi-articular limbs. Our results show that the disruptions of the movements caused by the velocity-dependent stretch reflexes are large, variable, and task-dependent enough to need inhibition, as has been proposed—but never quantified—by Sherrington and others [8, 19, 22, 29, 30]. We then demonstrate a generalizable spinal regulatory mechanism (similar to, but distinct from, $\alpha - \gamma$ co-activation) that significantly reduces disruptions caused by unregulated velocity-dependent stretch reflexes. Importantly, this mechanism is supported by homologous excitatory α -MN collaterals to γ -MNs that have been reported to exist among motoneurons [31, 32], but not thought to provide this function.

Muscle afferentation compels us to revisit the foundations of voluntary movement

The maxim apocryphally attributed to Sherrington that *'Inhibition is as important as excitation'* is emphasized in the iconic single-joint system with an agonist-antagonist muscle pair that customarily introduces students to the motor system [17, 33]. This neuromechanical system clearly shows that, for voluntary joint rotation to occur, the shortening of the 'agonist' muscle is made possible by the inhibition of length- and velocity-dependent stretch reflexes of the lengthening 'antagonist' muscle. As has been extensively documented in highly controlled experimental single-joint preparations, this can be made possible by propriospinal reciprocal inhibition or coordinated descending inhibitory signals [4, 18, 21, 29]. However, how this concept and its circuitry generalize for voluntary movement of realistic *multi-joint limbs with numerous multi-articular muscles* remains an open question in theories of motor control, and is left to specialists to grapple with [18, 21]. The reasons are multiple. For example, a same muscle can switch between eccentric and concentric contraction during a same movement, and the roles of agonist and antagonist lose their meaning [19, 20, 34]. *More fundamentally, the addition of muscle afferentation to the problem of motor control transforms muscle coordination into a mathematically over-determined problem (i.e., there is at most one solution: any eccentrically contracting muscle that fails to regulate its velocity-dependent stretch reflex can lock or disrupt the movement)* [19, 20]. This is the opposite of the traditional view that muscle coordination is mathematically redundant (i.e., *under-determined* where infinite combinations of muscle forces can produce a same joint torque). This dichotomy or apparent paradox arises because limbs are controlled by afferented musculotendons that can shorten and lengthen, making the control of joint rotations (i.e., limb motion) mechanically and neurophysiologically distinct from the control of net joint torques (i.e., limb forces) [19, 35, 36].

The issues raised by muscle afferentation are so profound that they have, broadly speaking, split the computational motor control community into two camps: those who seek to understand spinal circuitry and how muscle afferentation is regulated [5, 8, 18, 37–39], and those who assume that mechanism such as $\alpha - \gamma$ co-activation allow appropriate muscle lengthening as needed. As a result, muscle afferentation is not mentioned in canonical reviews of computational theories of motor control, or is assumed to be a form of feedback regulated at the cortical level via efferent copy and internal models [40–42]. Our results bridge both camps by providing fruitful research directions to the former, and objective quantification of the cost of not including muscle afferentation to the latter.

A humble low-level circuit to the rescue?

The main contribution of this work is that it confronts us with the previously unknown true cost of unmodulated velocity-dependent stretch reflexes, while also proposing an evolutionary and physiologically plausible solution at the level of propriospinal circuitry. Frankly, we were surprised by the magnitude and variety of types of disruptions that arose when velocity-dependent stretch reflexes are not modulated. In response to this we confirmed and made sure that in our simulations the maximal velocity-dependent stretch reflex gain was at a scale comparable to that seen in stretch reflexes in humans by Perrault and colleagues [28]. Importantly, the disruptive effect is consistently visible even when the gain is one tenth of the maximal gain (Figs.3A, 4A, and 5A). Moreover, we explored this effect in a total of 1,100 distinct movements. It was often the fact that the velocity-dependent stretch reflex emerged in the weakly excited muscles (Fig.7 and S2 Fig). Thus, we believe the disruptions we report are a realistic and valuable *computational* prediction of the neuromechanics of limb movement that are not possibly or easily obtained *experimentally*—which is one of the most useful applications of computational modeling [43].

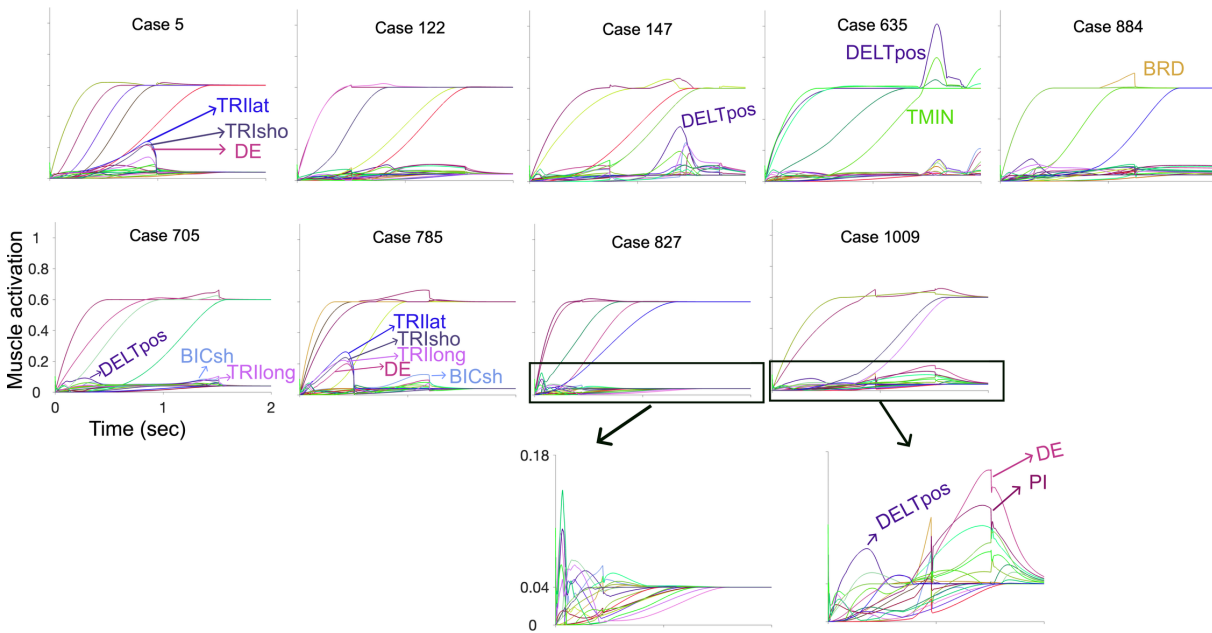


Fig 7. Sample muscle activation with velocity-dependent stretch reflex feedback at maximal reflex gain. Nine examples of α -MN -drive to muscles during closed-loop simulation with velocity-dependent stretch reflex at a reflex gain k of 10. Top plots are examples of cases shown in fig 3 in which scaling the velocity-dependent stretch reflex by the α -MN -drive to each muscle significantly reduced disruption in the movement trajectory and terminal position. Bottom plots are examples of cases shown in fig 4 that had large disruptions when the velocity-dependent stretch reflexes are scaled by the α -MN -drive to each muscle.

Our proposed mechanism simply scales velocity-dependent stretch reflex by an excitatory α -MN collateral. Such collateral projection among MNs have long been observed in studies of the cat spinal cord, Fig. 8A [31], but not interpreted in this context, or for this functional role. Rather, the functional role of that reported inter-motoneuronal facilitation was only speculated on and interpreted as connections between α -MNs . Importantly, those studies [31,32,44,45] did not specify or disprove that the excitatory (or disinhibitory) projections were from α -MNs to γ -MNs as we propose here. In addition to this evidence, recent studies in mice have shown recurrent excitation between MNs; with fast-type α -MN systematically receiving greater recurrent excitation than slow-type MNs [32,46]. Thus, prior studies partly support our proposed mechanism, even if their experimental limitations could not conclusively identify projections to γ -MNs . However, we believe that it is not unreasonable to suppose that such collateral projections to γ -MNs indeed exist. In addition, recent computational work also argues that Ia afferent signals for voluntary movement require fusimotor modulation independent of corticospinal drive [23]. We believe our mechanism provides this modulation. Experimental validation of our proposed circuit will require the maturation of some promising optogenetic techniques that could show such low-level control of γ -MN in all, or at least some, motoneuron pools in behaving animals [46–48].

165
166
167
168
169
170
171
172
173
174
175
176
177
178

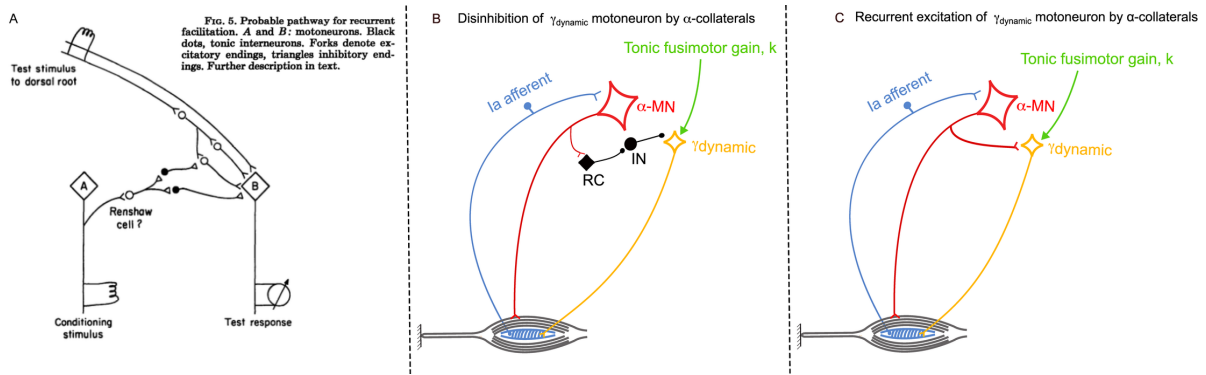


Fig 8. Three schematic spinal circuits compatible with Eqn. 2: From Wilson and Burgess (1962) [31] (left), its adaptation to have the collateral disinhibit the homologous γ -MN via a disynaptic projection via a Renshaw cell (middle), and a straightforward monosynaptic excitatory drive to the γ -MN compatible with [32] (right). All of these versions of collaterals from α -MN to γ -MN are able to achieve the results presented—yet they are neuroanatomically and functionally distinct from, and not equivalent to, $\alpha - \gamma$ co-activation (see Discussion).

It is important to note that our proposed spinal level mechanism for scaling $\gamma_{dynamic}$ MN activation by the homologous α -MN collateral is not only generalizable to any movement, but also independent of the cortical, subcortical or propriospinal competition at the presynaptic α -MN level. Rather, because it projects the actual (i.e., postsynaptic) α -MN drive to muscle fibers, this excitatory mechanism to the γ -MN sidesteps the uncertainty and delays arising from the presynaptic synthesis and competition among cortical, subcortical or propriospinal presynaptic projections to α -MN pools that $\alpha - \gamma$ co-activation must consider.

How does this low-level circuit compare with $\alpha - \gamma$ co-activation and other cortically-mediated variants?

The popular and dominant working hypotheses about the regulation of muscle spindle sensitivity [17, 49] revolve around the coordination between α -MN and γ -MN activity in a way that allows muscle proprioception and eccentric contractions. The traditional version of $\alpha - \gamma$ co-activation posits that the γ_{static} MNs that drive the intrafusal fibers of the secondary (II) spindle afferents (sensitive to muscle length) are activated synchronously with α -MNs. This prevents the intrafusal muscle fibers from going slack to maintain secondary spindle sensitivity. However, $\alpha - \gamma$ co-activation does not explicitly address the intrafusal primary Ia afferents involved in velocity-dependent stretch reflexes [50]. Other theories like *Fusimotor Setpoint* focus on Ia stretch-sensitivity during learning [14], but do not address arbitrary movements after they have been learned. Two other hypotheses posit that fusimotor drive is played out as a *Temporal Template* [51] or as *Goal-Directed Preparatory Control* [52].

Importantly, $\alpha - \gamma$ co-activation and its variants above hinge on the fundamental assumption that the system has sufficiently accurate knowledge of the time-varying variables that determine musculotendon lengths and velocities (e.g., the current and future states of all muscles, joint kinematics and external forces). Multiple theories have been proposed to provide such future knowledge (which is also needed for learning, error correction, response to perturbations, etc.) including efferent copy, internal models, optimal control, synergy control, and Bayesian estimation [41, 53–55]. However, time delays and uncertainty will always conspire to pollute such estimates and prevent time-critical coordination between homologous α - and γ -MN pools of a same muscle. In addition, there is the significant challenge of coordinating $\alpha - \gamma$ co-activation signals to arrive to their specific homologous pairs of α - and γ -MN pools via *different pathways with different conduction velocities* (i.e., predominantly cortico-spinal vs. reticulo-rubro- and vestibulo-spinal tracts, respectively). Lastly, any such synchronous control can only serve to bias the presynaptic input, but not directly provide the γ -MNs the actual postsynaptic α -MN drive to muscle fibers, as mentioned above.

In this work, we were careful to make an explicit comparison between our proposed circuit vs. the ideal implementation of $\alpha - \gamma$ co-activation (Fig. 2), as shown in Fig. 5. These results show that both approaches have functionally equivalent, but not identical, performance. This supports the face validity of $\alpha - \gamma$ co-activation that has been a fundamental tenet of sensorimotor neuroscience but, as mentioned above, is of uncertain implementation and

has multiple practical drawbacks. We conclude that, given their arguably equivalent performance, Occam's Razor strongly encourages us to favor the simplicity of a low-level circuit to modulate γ -MNs via α -MN collaterals as shown in Fig. 8, which inherently sidesteps the challenges of time delays, uncertainty and presynaptic competition of any version of $\alpha - \gamma$ co-activation .

Locally-mediated modulation of γ -MNs via α -MN collaterals enables meaningful cerebellar and cortical learning and adaptation mechanisms

Biological and machine learning have the fundamental requirement that the system in question be minimally controllable, observable and predictable [56]. Said differently, *meaningful error signals* are necessary for any effective and efficient learning processes. Our results for unmodulated velocity-dependent stretch reflexes for voluntary movement show that a realistic limb with afferented muscles will have disruptions that are movement-specific, typically large and variable, and that could even change movement direction as the velocity-dependent reflex gain increases. Therefore, the presence of unmodulated velocity-dependent stretch reflexes presents any learning strategy with error signals that are at best highly nonlinear, and at worst not meaningful for learning—making it difficult or even impractical to learn limb movements from a naïve state. Placing our results in the context of the rich literature on motor learning and control, and using cerebellar circuits as an example, we argue that the regulatory effects the proposed circuit in fact serve as a critical enabler for learning. Current thinking is that computational frameworks of the cerebellum favor hierarchical reinforcement learning with predictions via multiple internal models [42]. However, forming, refining and exploiting an internal model of any variety from a naïve state requires experience with a minimally controllable, observable and predictable system. We propose that this low-level circuit for locally-mediated modulation of γ -MNs via α -MN collaterals regularizes any new voluntary limb movement to the point that it can *enable learning* from a naïve state by combining motor babbling [57] or directed practice [58] with a higher-level learning strategy. It is to the advantage of the individual to be born with a body that is minimally controllable from the start.

Importantly, and as can be seen from the measurable cumulative and terminal errors in Fig.5B, this low-level circuit is far from a panacea, but is simply a means to mitigate the severe nonlinearities of the afferented limb. This leaves much room, and need, for improvement via supraspinal mechanisms. Nevertheless, this low-level circuit then serves as 'training wheels' that enable exploration-exploitation during the formation of an internal model (or Bayesian priors, synergies, gradient-descent strategies, etc. if the reader is not of the internal-model persuasion [53]). From an evolutionary perspective, we could even speculate that such a low-level circuit is an ancient enabler of movement when the primeval β skeleto-fusimotor MNs in amphibians and reptiles were superseded by separate α - and γ -MNs in mammals [59]—and the need arose for some form of α - γ coordination.

We speculate that, like β -MNs, the proposed circuit is the *afferentation Yin* that complements the *efferentation Yang* of Hennemann's Size Principle to enable low-level, robust regulation of graduated movement. Such fundamental and complementary low-level pair of circuits in a hierarchical and distributed nervous system [5] would then provide local and robust regulation of muscle force for voluntary movement without the need for higher level centers at first—but which can then evolve other more sophisticated cortically-mediate mechanisms to modulate, adapt, supersede or even replace that functionality. In fact, as ontogeny recapitulates phylogeny, such a regulator of velocity-dependent stretch reflex during an individual's early development in an individual would then in time be modulated, after corticospinal myelination [60], when sophisticated controllers become available such as those reported and intensely studied for cerebellar control of movement [42].

Limitations and future work

The scope of this computational study is limited to the investigation of the disruption of voluntary movement caused by velocity-dependent stretch reflex from Ia afferent nerve fibers. Our spindle model is an over-simplified version of previously described models [7, 61, 62]. Moreover, we assume that there is appropriate γ_{static} drive that keeps the muscle spindle from going slack, and thus do not consider stretch reflex signals from II afferents [18, 21]. However, it is conceptually straightforward to consider that such collateral can just as easily project to γ_{static} MNs to accomplish the putative goal of $\alpha - \gamma$ co-activation to prevent slacking of the intrafusal fibers that keep the muscles spindles active. Future work will complete our investigations of the fusimotor system. Similarly, we use a simple Hill-type muscle model included in MuJoCo, which can be improved by our recent work [63].

Despite these simplifications, and without lack of generality, our result shows the invariably disruptive effect of unmodulated pure velocity-dependent stretch reflex on voluntary movement at different fusimotor dynamic gains (i.e., stretch reflex gains). In this study we did not intend to represent the full fusimotor system and spinal circuitry; rather we sought to, as a first step, isolate the effects of pure velocity signal from Ia afferent on voluntary movement. Lastly, we necessarily present the best-case scenario for the mitigation of cumulative and terminal errors as we do not consider mono- and di-synaptic time delays in our propose modulation of γ -MN activity. However, this is also an unexplored and unresolved issue in $\alpha - \gamma$ co-activation and its variants as mentioned above. Future work can address conduction and computational delays, as well as nonlinearities and delays from recruitment and rate-coding, muscle activation-contraction dynamics [64], etc.

From a behavioral perspective, our simulated tasks are not meant represent a specific task-related upper limb movements such as reaching or joint flexion/extension [20, 23, 28, 30, 37]. Rather, we start with open-loop arm movements that explore and exploit the full 3D workspace so as to ask the fundamental question of the effects of disruptions from velocity-dependent stretch reflex in general. Nevertheless, it is worth considering whether the effects of velocity-dependent stretch reflexes on the simulated movements can extend to movements of functional importance for humans, and especially reaching movements compromised by pathologic synergies in neurological conditions such as stroke, or tremor in Parkinson's disease. For this, it will be necessary to incorporate more detailed models of the muscle spindle, spinal circuitry, and tasks relevant to human functions—and of the neuropathology of interest.

Funding

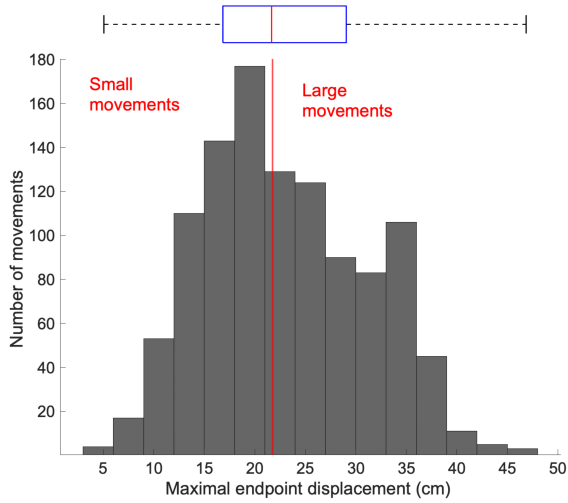
This work is supported in part by the NIH (R01 AR-050520, R01 AR-052345 and R21-NS113613), DOD CDMRP Grant MR150091, DARPA-L2M program Award W911NF1820264, NSF CRCNS Japan-US 2113096 to FV-C, and a fellowships from the USC Viterbi School of Engineering to GN and LA. The content is solely the responsibility of the authors and does not necessarily represent the official views of the NIH, NSF, DoD, or DARPA.

Acknowledgments

The authors would like to thank Junhyuck Woo for his assistance with initial development of the computational model in MuJoCo in the course BME 504, and Dr. Kazuhiko Seki and Dr. Gerald Loeb for their insightful discussion of this work.

Supporting Material

287

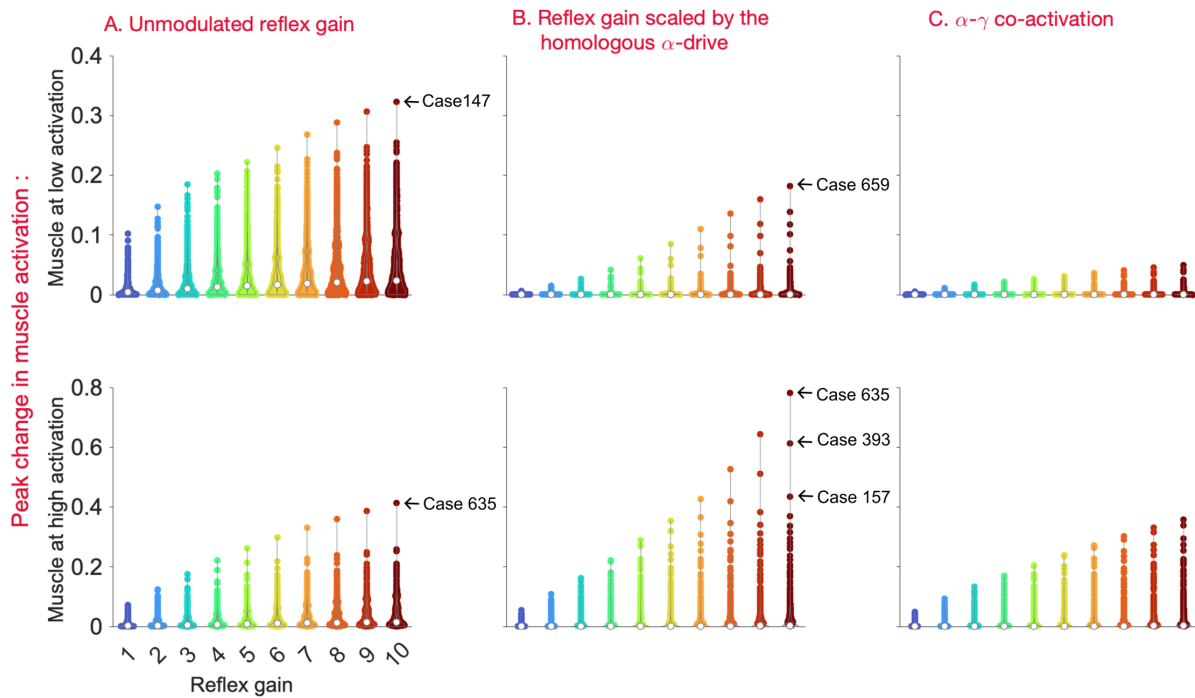


288

S1 Fig. Distribution of maximal endpoint displacement of the reference trajectories of the open-loop movements.

289

290



291

S2 Fig. Distribution of the peak change in the muscle activations for all 1,100 cases at each reflex gain.

292

293

References

1. Proske U, Gandevia SC. Kinesthetic senses. *Comprehensive Physiology*. 2011;8(3):1157–1183.
2. Proske U, Gandevia SC. The proprioceptive senses: their roles in signaling body shape, body position and movement, and muscle force. *Physiological reviews*. 2012;.
3. Strzalkowski ND, Peters RM, Inglis JT, Bent LR. 50 Years of Microneurography: Insights into Neural Mechanisms in Humans: Cutaneous afferent innervation of the human foot sole: what can we learn from single-unit recordings? *Journal of Neurophysiology*. 2018;120(3):1233.
4. Sherrington CS. Reflex inhibition as a factor in the co-ordination of movements and postures. *Quarterly Journal of Experimental Physiology: Translation and Integration*. 1913;6(3):251–310.
5. Loeb GE, Brown IE, Cheng EJ. A hierarchical foundation for models of sensorimotor control. *Experimental brain research*. 1999;126:1–18.
6. Proske U. The mammalian muscle spindle. *Physiology*. 1997;12(1):37–42.
7. Mileusnic MP, Brown IE, Lan N, Loeb GE. Mathematical models of proprioceptors. I. Control and transduction in the muscle spindle. *Journal of neurophysiology*. 2006;96(4):1772–1788.
8. Jaleddini K, Niu CM, Raja SC, Sohn WJ, Loeb GE, Sanger TD, et al. Neuromorphic meets neuromechanics, part II: the role of fusimotor drive. *Journal of neural engineering*. 2017;14(2):025002.
9. Sanger TD, Chen D, Fehlings DL, Hallett M, Lang AE, Mink JW, et al. Definition and classification of hyperkinetic movements in childhood. *Movement Disorders*. 2010;25(11):1538–1549.
10. Krakauer JW, Carmichael ST. *Broken movement: the neurobiology of motor recovery after stroke*. MIT Press; 2022.
11. Lund J, Smith A, Sessle B, Murakami T. Activity of trigeminal alpha-and gamma-motoneurons and muscle afferents during performance of a biting task. *Journal of Neurophysiology*. 1979;42(3):710–725.
12. Edin BB, Vallbo A. Stretch sensitization of human muscle spindles. *The Journal of physiology*. 1988;400(1):101–111.
13. Ribot E, Roll J, Vedel J. Efferent discharges recorded from single skeletomotor and fusimotor fibres in man. *The Journal of Physiology*. 1986;375(1):251–268.
14. Prochazka A. Proprioceptive feedback and movement regulation. *Comprehensive Physiology*. 2010; p. 89–127.
15. Yaron A, Kowalski D, Yaguchi H, Takei T, Seki K. Forelimb force direction and magnitude independently controlled by spinal modules in the macaque. *Proceedings of the National Academy of Sciences*. 2020;117(44):27655–27666.
16. Macefield VG, Knellwolf TP. Functional properties of human muscle spindles. *Journal of neurophysiology*. 2018;120(2):452–467.
17. Kandel ER, Schwartz JH, Jessell TM, Siegelbaum S, Hudspeth AJ, Mack S, et al. *Principles of neural science*. vol. 4. McGraw-hill New York; 2000.
18. Pierrot-Deseilligny E, Burke D. *The circuitry of the human spinal cord: its role in motor control and movement disorders*. Cambridge university press; 2005.
19. Valero-Cuevas FJ. *Fundamentals of neuromechanics*. vol. 8. Springer; 2016.
20. Hagen DA, Valero-Cuevas FJ. Similar movements are associated with drastically different muscle contraction velocities. *Journal of biomechanics*. 2017;59:90–100.

21. Windhorst U. Spinal Cord Circuits: Models and Reality. *Neurophysiology*. 2021;53(3):142–222.
22. Berry JA, Marjaninejad A, Valero-Cuevas FJ. Edge Computing in Nature: Minimal pre-processing of multi-muscle ensembles of spindle signals improves discriminability of limb movements. *Frontiers in Physiology*. 2023;14:1183492.
23. Hardesty RL, Boots MT, Yakovenko S, Gritsenko V. Computational evidence for nonlinear feedforward modulation of fusimotor drive to antagonistic co-contracting muscles. *Scientific Reports*. 2020;10(1):10625.
24. Chan SS, Moran DW. Computational model of a primate arm: from hand position to joint angles, joint torques and muscle forces. *Journal of neural engineering*. 2006;3(4):327.
25. Delp SL, Anderson FC, Arnold AS, Loan P, Habib A, John CT, et al. OpenSim: open-source software to create and analyze dynamic simulations of movement. *IEEE transactions on biomedical engineering*. 2007;54(11):1940–1950.
26. Ikkala A, Hämäläinen P. Converting biomechanical models from opensim to Mujoco. In: *International Conference on NeuroRehabilitation*. Springer; 2020. p. 277–281.
27. Todorov E, Erez T, Tassa Y. Mujoco: A physics engine for model-based control. In: *2012 IEEE/RSJ international conference on intelligent robots and systems*. IEEE; 2012. p. 5026–5033.
28. Krutky MA, Ravichandran VJ, Trumbower RD, Perreault EJ. Interactions between limb and environmental mechanics influence stretch reflex sensitivity in the human arm. *Journal of neurophysiology*. 2010;103(1):429–440.
29. Sherrington CS, et al. Inhibition as a coordinative factor. N Foundation (Ed), Nobel Lectures, Physiology and Medicine. 1932; p. 278–289.
30. Sandbrink KJ, Mamidanna P, Michaelis C, Bethge M, Mathis MW, Mathis A. Contrasting action and posture coding with hierarchical deep neural network models of proprioception. *Elife*. 2023;12:e81499.
31. Wilson VJ, Burgess PR. Disinhibition in the cat spinal cord. *Journal of Neurophysiology*. 1962;25(3):392–404.
32. Beato M, Bhumbra G. Synaptic Projections of Motoneurons Within the Spinal Cord. In: *Vertebrate Motoneurons*. Springer; 2022. p. 151–168.
33. Enoka RM. *Neuromechanics of human movement*. Human kinetics; 2008.
34. Valero-Cuevas FJ, Cohn B, Yngvason H, Lawrence EL. Exploring the high-dimensional structure of muscle redundancy via subject-specific and generic musculoskeletal models. *Journal of biomechanics*. 2015;48(11):2887–2896.
35. Chib VS, Krutky MA, Lynch KM, Mussa-Ivaldi FA. The separate neural control of hand movements and contact forces. *Journal of Neuroscience*. 2009;29(12):3939–3947.
36. Venkadesan M, Valero-Cuevas FJ. Neural control of motion-to-force transitions with the fingertip. *Journal of Neuroscience*. 2008;28(6):1366–1373.
37. Raphael G, Tsianos GA, Loeb GE. Spinal-like regulator facilitates control of a two-degree-of-freedom wrist. *Journal of Neuroscience*. 2010;30(28):9431–9444.
38. Niu CM, Jalaleddini K, Sohn WJ, Rocamora J, Sanger TD, Valero-Cuevas FJ. Neuromorphic meets neuromechanics, part I: the methodology and implementation. *Journal of neural engineering*. 2017;14(2):025001.
39. Takei T, Seki K. Spinal premotor interneurons mediate dynamic and static motor commands for precision grip in monkeys. *Journal of Neuroscience*. 2013;33(20):8850–8860.

40. Scott SH. Optimal feedback control and the neural basis of volitional motor control. *Nature Reviews—Neuroscience*. 2004;5:535.
41. Todorov E, Jordan MI. Optimal feedback control as a theory of motor coordination. *Nature neuroscience*. 2002;5(11):1226–1235.
42. Kawato M, Ohmae S, Hoang H, Sanger T. 50 years since the Marr, Ito, and Albus models of the cerebellum. *Neuroscience*. 2021;462:151–174.
43. Valero-Cuevas FJ, Hoffmann H, Kurse MU, Kutch JJ, Theodorou EA. Computational models for neuromuscular function. *IEEE reviews in biomedical engineering*. 2009;2:110–135.
44. Cullheim S, Kellerth JO, Conradi S. Evidence for direct synaptic interconnections between cat spinal α -motoneurons via the recurrent axon collaterals: a morphological study using intracellular injection of horseradish peroxidase. *Brain research*. 1977;132(1):1–10.
45. Cullheim S, Fleshman J, Glenn L, Burke R. Three-Dimensional architecture of dendritic trees in type-identified α -motoneurons. *Journal of Comparative Neurology*. 1987;255(1):82–96.
46. Bhumbra GS, Beato M. Recurrent excitation between motoneurons propagates across segments and is purely glutamatergic. *PLoS biology*. 2018;16(3):e2003586.
47. Chopek JW, Nascimento F, Beato M, Brownstone RM, Zhang Y. Sub-populations of spinal V3 interneurons form focal modules of layered pre-motor microcircuits. *Cell Reports*. 2018;25(1):146–156.
48. Chalif JI, de Lourdes Martínez-Silva M, Pagiazitis JG, Murray AJ, Mentis GZ. Control of mammalian locomotion by ventral spinocerebellar tract neurons. *Cell*. 2022;185(2):328–344.
49. Wikipedia contributors. Muscle spindle — Wikipedia, The Free Encyclopedia; 2023. Available from: https://en.wikipedia.org/w/index.php?title=Muscle_spindle&oldid=1173583463.
50. Vallbo A, al Falahe NA. Human muscle spindle response in a motor learning task. *The Journal of Physiology*. 1990;421(1):553–568.
51. Taylor A, Durbaba R, Ellaway P, Rawlinson S. Static and dynamic γ -motor output to ankle flexor muscles during locomotion in the decerebrate cat. *The Journal of physiology*. 2006;571(3):711–723.
52. Papaioannou S, Dimitriou M. Goal-dependent tuning of muscle spindle receptors during movement preparation. *Science Advances*. 2021;7(9):eabe0401.
53. Cohn BA, Szedlák M, Gärtner B, Valero-Cuevas FJ. Feasibility theory reconciles and informs alternative approaches to neuromuscular control. *Frontiers in computational neuroscience*. 2018;12:62.
54. Körding KP, Wolpert DM. Bayesian integration in sensorimotor learning. *Nature*. 2004;427(6971):244–247.
55. Tresch MC, Jarc A. The case for and against muscle synergies. *Current opinion in neurobiology*. 2009;19(6):601–607.
56. Kudithipudi D, Aguilar-Simon M, Babb J, Bazhenov M, Blackiston D, Bongard J, et al. Biological underpinnings for lifelong learning machines. *Nature Machine Intelligence*. 2022;4(3):196–210. doi:10.1038/s42256-022-00452-0.
57. Marjaninejad A, Urbina-Meléndez D, Cohn BA, Valero-Cuevas FJ. Autonomous functional movements in a tendon-driven limb via limited experience. *Nature machine intelligence*. 2019;1(3):144–154.
58. Steele CJ, Zatorre RJ. Practice makes plasticity. *Nature Neuroscience*. 2018;21(12):1645–1646.
59. Manuel M, Zytnicki D. Alpha, beta and gamma motoneurons: functional diversity in the motor system’s final pathway. *Journal of integrative neuroscience*. 2011;10(03):243–276.

60. Kinney HC, Volpe JJ. Myelination events. In: Volpe's neurology of the newborn. Elsevier; 2018. p. 176–188.
61. Tsianos GA, Goodner J, Loeb GE. Useful properties of spinal circuits for learning and performing planar reaches. *Journal of neural engineering*. 2014;11(5):056006.
62. Nagamori A, Laine CM, Valero-Cuevas FJ. Cardinal features of involuntary force variability can arise from the closed-loop control of viscoelastic afferented muscles. *PLoS computational biology*. 2018;14(1):e1005884.
63. Nagamori A, Laine CM, Loeb GE, Valero-Cuevas FJ. Force variability is mostly not motor noise: Theoretical implications for motor control. *PLoS Computational Biology*. 2021;17(3):e1008707.
64. Cohn BA, Valero-Cuevas FJ. Muscle redundancy is greatly reduced by the spatiotemporal nature of neuromuscular control. *Frontiers in Rehabilitation Sciences*. 2023;4.